Journal of Ceramic Processing Research. Vol. 13, Special. 2, pp. s295~s299 (2012)

J O U R N A L O F
Ceramic
Processing Research

Comparative study of InGaN/GaN multi-quantum wells in polar (0001) and semipolar (11-22) GaN-based light emitting diodes

Ki-Ryong Song, Dong-Sub Oh, Min-Jae Shin and Sung-Nam Lee*

Department of Nano-Optical Engineering, Korea Polytechnic University, Siheung, Gyeonggi-Do 429-793, Korea

We investigated the crystal and the optical properties of GaN-based blue light emitting diodes (LEDs) which were simultaneously grown on c-plane (0001) and semipolar (11-22) GaN templates by using metal-organic chemical vapor deposition (MOCVD). The X-ray rocking curves (XRCs) full width at half maximums (FWHMs) of c-plane (0001) and semipolar (11-22) GaN templates were 275 and 889 arcsec, respectively. In addition, high-resolution X-ray ω-2θ scan showed that satellite peaks of semipolar (11-22) InGaN quantum-wells (QWs) was weaker and broader than that of c-plane (0001) InGaN QWs, indicating that the interface quality of c-plane (0001) QWs was superior to that of semipolar (11-22) QWs. Photoluminescence (PL) and electroluminescence (EL) results showed that the emission intensity and the FWHMs of polar c-plane (0001) LED were much higher and narrower than those of semipolar (11-22) LED, respectively. From these results, we believed that relative poor crystal quality of semipolar (11-22) GaN template might give rise to the poor interfacial quality of QWs, resulting in lower output power than conventional c-plane (0001) GaN-based LEDs.

Key words: GaN, Polar, Semipolar, LED, MOCVD.

Introduction

III-nitride semiconductors have been used for growth of light emitting devices such as light emitting diodes (LEDs) and laser diodes (LDs), etc. [1]. In general, GaN-based optoelectronic devices are predominantly grown in c-plane (0001) orientation. However, there are important physical problems to achieve high power LD/LEDs, which are quantum confinement stark effect due to their spontaneous and piezoelectric polarizations fields [2]. It was reported that the limits of emission efficiency for conventional c-plane (0001) GaN-based LEDs could be overcome by using semipolar or nonpolar GaN films which represented small or no polarization effects, respectively [3]. Therefore, nonpolar and semipolar GaN-based LED/LDs represented less blueshift and higher emission efficiency with increasing the injection current [4].

However, heteroepitaxial semipolar (11-22) GaN films have been still suffered from poor crystal quality and arrowhead-like surface structures because of anisotropic crystallographic mismatch between semipolar (11-22) GaN and m-plane (10-10) sapphire, as shown in Fig. 1. It is often reported that semipolar (11-22) GaN grown on m-plane (10-10) sapphire had poor crystal qualities with threading dislocations (TDs) of ~ 10^{10}/cm^2 and basal stacking faults (BSFs) of ~ 10^5/cm [5], which could be acted as non-radiative recombination centers. To achieve high performance semipolar (11-22) InGaN/GaN quantum wells (QWs) LEDs to exceed polar (0001) InGaN/GaN QWs LEDs, the growth mechanism and the optical properties of semipolar (11-22) InGaN/GaN QWs should be fully understood. However, there are only a few systematic reports to compare polar c-plane (0001) with semipolar (11-22) GaN-based LED structure. This work aims to comparatively investigate the crystal and optical properties of LEDs with blue InGaN/GaN quantum-wells (QWs) structures grown on polar c-plane (0001) and semipolar (11-22) GaN templates.

Experimental

Metalorganic chemical vapor deposition (MOCVD) was used to grow polar c-plane (0001) and semipolar (11-22) GaN on c-plane (0001) and m-plane (10-10) sapphire substrates, respectively. 2.0 μm-thick semipolar (11-22) GaN and polar c-plane (0001) GaN templates were prepared. Polar c-plane (0001) GaN template was grown by conventional two-step growth, while semipolar (11-22) GaN templates were grown by novel one-step growth method [6]. Un-doped semipolar (11-22) GaN templates were deposited at 1060 °C and 200 torr with a V/III ratio of 1950, which was optimum growth condition in our experiment to minimize arrowhead-like surface structure. After that, both templates were simultaneously loaded into MOCVD reactor to grow GaN-based blue LED structures, which consisted of 3.0 μm-thick Si-doped n-type GaN, five-period 4.0 nm-thick InGaN wells/10.0 nm-thick GaN barriers and 0.1 μm-thick Mg-doped p-type GaN layer. In addition, to analyze the surface morphology of active layer, we

*Corresponding author:
Tel : +82-31-8041-0721
Fax: +82-31-8041-0729
E-mail: snlee@kpu.ac.kr

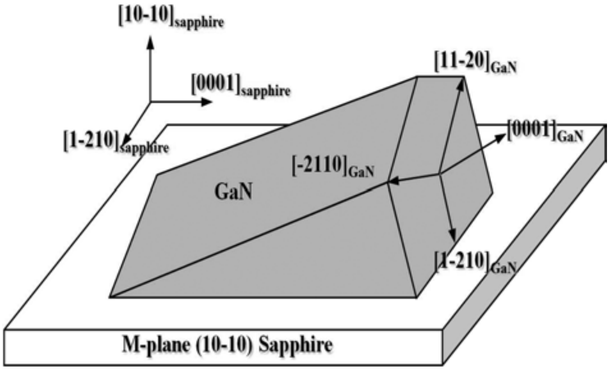

Fig. 1. A schematic epitaxial direction between semipolar (11-22) GaN and m-plane (10-10) sapphire substrate.

grew only polar c-plane (0001) and semipolar (11-22) InGaN/GaN QWs grown on both templates.

The microscopic surface morphology was analyzed by atomic force microscopy (AFM). The crystal quality of both GaN templates and the interfacial quality of both InGaN QWs were characterized by high-resolution X-ray diffraction (HR-XRD) with different incident beam directions of [1-100] and [11-2-3]. And, the optical properties of polar (0001) and semipolar (11-22) GaN-based LEDs with InGaN/GaN QWs were characterized by room temperature photoluminescence (PL) and electroluminescence (EL) analysis. EL measurements were performed by forming In dots as n-type and p-type contact metals on both LED wafers. For PL measurement, both samples were focused by the 325 nm line of He-Cd laser with the beam diameter of 20 μm and the excitation power of 1.0 kW/cm^2.

Results and Discussion

Figs. 2 (a) and (b) showed AFM images of c-plane (0001) and semipolar (11-22) GaN grown on c-plane (0001) and m-plane (10-10) sapphire substrates, respectively. The microscopic surface morphology of c-plane (0001) GaN template represented the typical step-like surface structure, whereas that of semipolar (11-22) GaN template showed the arrowhead-like surface which would be dependent on growth conditions such as growth temperature, pressure and V/III ratio [7-8]. It is well known that anisotropic surface structure of semipolar (11-22) GaN may be caused by the incorporation probability and the diffusion length of Ga and N adatoms on film surface toward anisotropic crystallographic directions such as [11-2-3] and [1-100] due to the crystallographic difference between m-plane (10-10) sapphire and semipolar (11-22) GaN [9], as shown in Fig. 1. However, the macroscopic surface morphology of semipolar (11-22) GaN template was mirror-like surface comparable to c-plane (0001) GaN template not shown in here. It indicated that the surface of semipolar (11-22) GaN was smooth enough to grow LED structure. Figs. 2 (c) and (d) showed AFM images

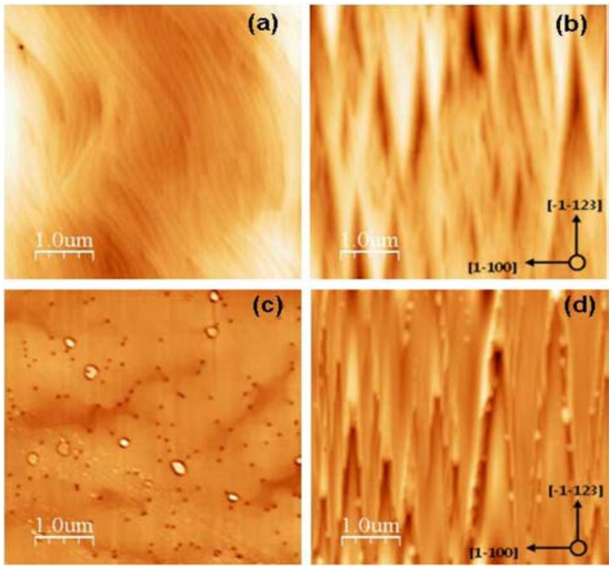

Fig. 2. AFM images (5 μm × 5 μm) of (a) polar c-plane (0001) GaN, (b) semipolar (11-22) GaN template, (c) polar c-plane (0001) and (d) semipolar (11-22) InGaN QWs structure.

of c-plane (0001) and semipolar (11-22) InGaN/GaN QWs structure, respectively. The microscopic surface of c-plane (0001) InGaN/GaN QWs represented the typical spiral structures with some V-shape pits [10], while that of semipolar (11-22) InGaN/GaN QWs showed the arrowhead-like surface structure. In addition, there is no any V-shape pit on the surface of semipolar (11-22) InGaN QWs. In general, it has been reported that surface V-shape pits would be developed by low surface migration of Ga adatoms and stress accumulation during the relative low temperature growth (< 800 °C) of c-plane (0001) InGaN QWs [10]. Therefore, the anisotropic internal stress was thought to be relaxed by the more generation of arrowhead-like surface instead of the formation of surface V-shape pits on the contrary to c-plane (0001) during the growth of semipolar (11-22) InGaN QWs [11]. In addition, root-mean-square (RMS) roughness of c-plane (0001) and semipolar (11-22) InGaN QWs were 1.1 nm and 5.2 nm, respectively. These results would explain that the surface morphology of semipolar (11-22) InGaN QWs was roughened by developing arrowhead-like surface structure without the generation of V-shape defects, resulting in the similar surface of semipolar (11-22) GaN template [12].

The crystal and interfacial qualities of c-plane (0001) and semipolar (11-22) LED structures were characterized by the HR-XRD measurements. Figs. 3 (a) and (b) showed ω-rocking curve of c-plane (0001) and semipolar (11-22) GaN templates, respectively. The X-ray rocking curves (XRCs) full width at half maximums (FWHMs) of c-plane (0001) GaN template was 275 arcsec for the direction of $[11\text{-}20]_{GaN}$, while that of semipolar (11-22) GaN was 889 arcsec for the direction of $[11\text{-}2\text{-}3]_{GaN}$. It indicated that the crystal

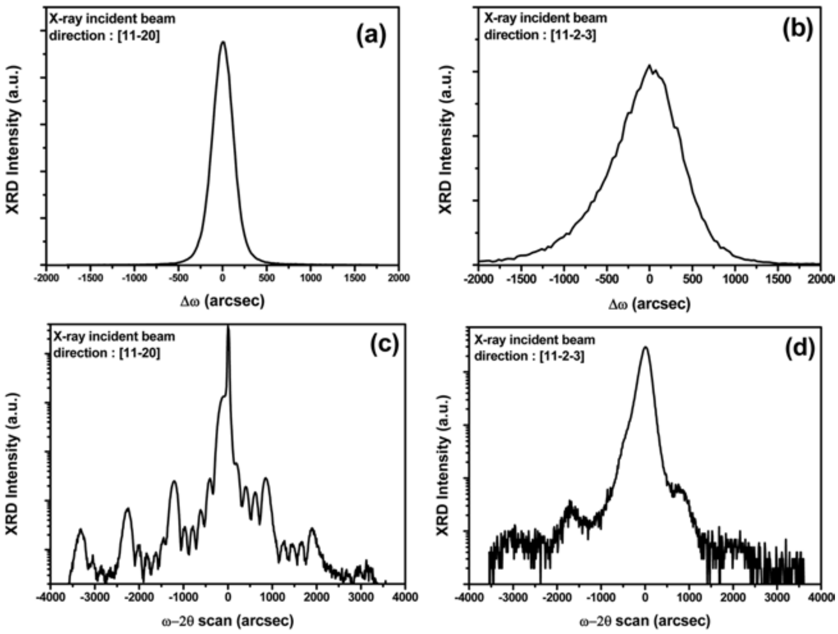

Fig. 3. X-ray rocking curves for (a) polar c-plane (0001) GaN and (b) (11-22) GaN templates. HR-XRD ω-2θ scans of (c) polar c-plane (0001) and (d) semipolar (11-22) LEDs with InGaN/GaN QWs.

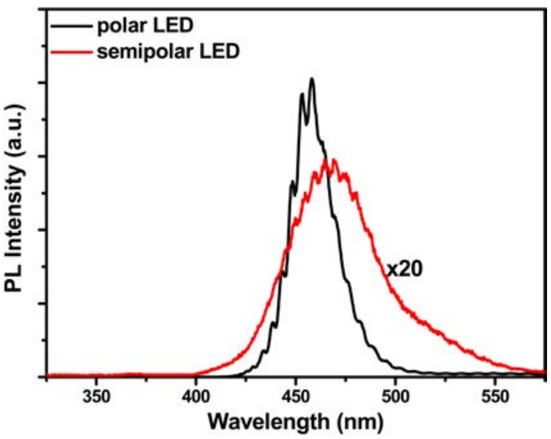

Fig. 4. Room temperature PL spectra of polar c-plane (0001) and semipolar (11-22) LEDs with InGaN/GaN QWs structure. (PL spectrum of semipolar (11-22) GaN-LED was multiplied by 20 times.)

quality of semipolar (11-22) GaN template was still poorer than that of polar c-plane (0001) GaN. Relative poor crystal quality of semipolar (11-22) GaN template was caused by generating a lots crystal defects such as TDs of ~ $10^{10}/cm^2$ and BSF of ~ 10^5/cm due to the large anisotropic lattice mismatch between semipolar (11-22) GaN and m-sapphire [13-14]. In spite of the large mismatch between semipolar (11-22) GaN and m-plane (10-10) sapphire, it is believed that the possible reason of epitaxial growth was our optimum growth conditions which favor long diffusion length, high temperatures, low growth rates and low growth pressures, resulting in the formation of (11-22) GaN, and indicating that this is the orientation closer to equilibrium [15]. Figs. 3 (c) and (d) showed the results of ω-2θ scans for c-plane (0001) and semipolar (11-22) LED structure, respectively. The satellite peaks of c-plane (0001) InGaN/GaN QWs was clearly developed, whereas those of semipolar (11-22) InGaN/GaN QWs was much weak and broad, indicating that the interfacial quality and the periodicity of c-plane (0001) InGaN/GaN QWs was superior to that of semipolar (11-22) InGaN/GaN QWs. As shown in the surface analysis, the surface of semipolar (11-22) InGaN QW was much poorer than that of polar c-plane (0001) GaN, which was consistent with the poor interfacial quality of semipolar (11-22) InGaN/GaN QW [16]. These results cold suggest that the poor surface and crystal quality of semipolar (11-22) GaN template could significantly affect the deterioration of interface quality during the growth of InGaN/GaN QWs [17].

Fig. 4 showed the room temperature PL spectra of polar c-plane (0001) and semipolar (11-22) LEDs with InGaN/GaN QWs structure. The PL emission wavelength of semipolar (11-22) LED was 467.8 nm which was longer than that 456.9 nm of polar LED. PL FWHMs of polar and semipolar (11-22) LEDs were 19.4 and 34.4 nm, respectively. It indicated that the distribution of In atoms in semipolar (11-22) InGaN QWs was much less uniformity than polar c-plane (0001) InGaN QWs, resulting in longer and broader emission spectrum due to the In localization states. In addition, PL intensity of polar LED was 22 times higher than that of semipolar (11-22) LED. The random distribution of the In-rich region may influence the long-wavelength absorption of the whole InGaN layer, absorption and scattering by the In-rich region, which reduces the transmission of the photons. It is a rather easy way for them to recombine in deep levels. When the excited carriers are trapped by In-rich QDs, they have no choice but to

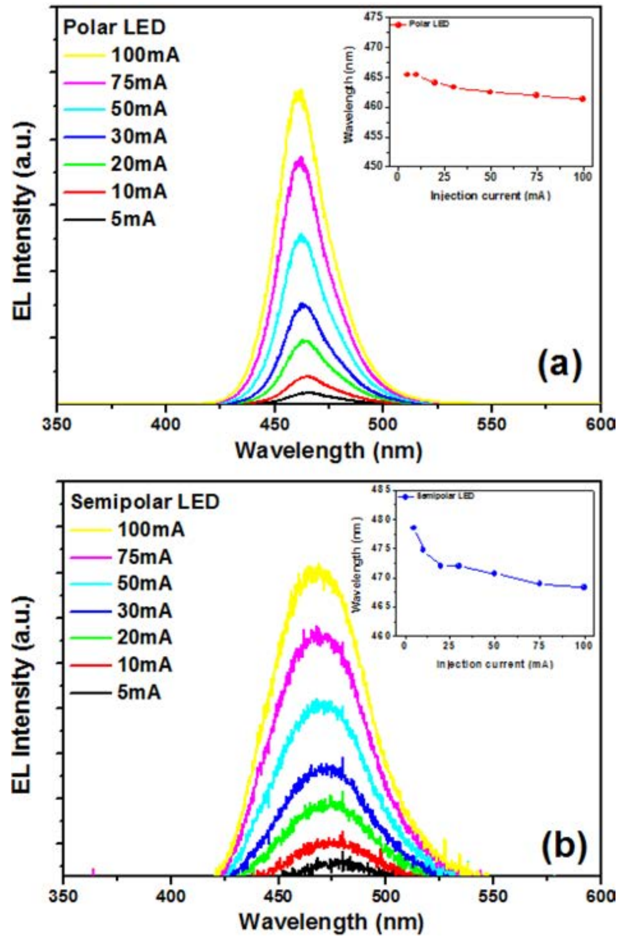

Fig. 5. EL spectra of (a) polar c-plane (0001) LED and (b) semipolar (11-22) LED with increasing the injection current. Each insets are the emission peak shifts of polar and semipolar (11-22) LED as a function of injection current.

radiative recombination. The absolute decreases for both emissions with the increase in x are due to the lattice defects like non-radiative levels and weak confinement of In-rich regions for trapped carriers. The increases of In composition will cause severe InGaN phase separation, which will broaden the InGaN peaks [18]. Therefore, it can be explained that low PL intensity of semipolar (11-22) InGaN QWs would be attributed to a lots crystal defects such as TDs and BSFs around In localization regions, which was consistent with the results of EL measurements [19].

Figs. 5 (a) and (b) showed that EL spectra of polar (0001) and semipolar (11-22) LEDs with increasing injection current from 5 to 100 mA. The emission wavelengths of polar and semipolar (11-22) LED were 464 and 472.5 nm at the injection current of 20 mA. EL intensity of polar LED was much higher than that of semipolar (11-22) LED, which was similar trend with PL measurement as shown in Fig. 4. As shown in Figs. 3 (a) and (b), the crystal quality of semipolar (11-22) GaN template was still poorer than that of polar c-plane (0001) GaN. From the analysis of satellite peaks in Figs 3 (c) and (d), the interfacial quality of polar QWs was much better than that of semipolar (11-22) QWs [20-21]. Therefore, the poor optical quality of semipolar (11-22) LED would be ascribed to lots crystal defects and poor interfacial qualities as non-radiative recombination centers [22]. Insets represented the emission peak shift of polar and semipolar (11-22) LEDs as a function of injection current from 5 to 100 mA. It can be seen that the blueshifts of EL peak position for polar and semipolar (11-22) LEDs were measured by 4.01 and 10.25 nm, respectively. Assuming that there was no piezoelectric polarization field in semipolar (11-22) InGaN/GaN QW region, the higher blueshift of semipolar (11-22) LED would be ascribed to the only band-filling effect on high In localization states [23]. It would be caused by the crystal quality of semipolar (11-22) GaN templates and the interfacial quality of InGaN/GaN QWs. For this reason, the In localization states were easily appeared in poor crystal quality and interfacial quality region of semipolar (11-22) InGaN/GaN QWs [24]. It was consistent with the result of PL and EL measurement. In addition, EL FWHMs of semipolar (11-22) QWs was twice broader than that of polar (0001) QWs. It may be caused by In phase separation around crystal and interfacial defects in semipolar (11-22) InGaN/GaN QWs region [25]. In particular, the band-tail states are formed in local potential minima like quantum dots (QDs). Their origin could be assigned to various causes, such as composition fluctuations, high density of impurity states, and inhomogeneous lattice deformations, etc. In InGaN system, the formation of band-tail states may arise from fluctuations of In content, often observed in InGaN/GaN QW samples. Such In phase segregation would create local potential fluctuations that are highly susceptible to rapid state filling as the excitation level is increased [26]. Therefore, this effect can be attributed to the rapid band filling of localized $In_xGa_{1-x}N$ radiative centers composed of large In concentrations. The deeper localized potential fluctuations are highly susceptible to rapid state filling as the excitation level is increased [27].

Conclusions

We investigated the structural and the optical properties of polar c-plane (0001) and semipolar (11-22) GaN-based LEDs with blue InGaN/GaN QWs structure. The surface morphology of polar InGaN QWs was typical spiral structures with some pits, while that of semipolar (11-22) InGaN QWs was arrowhead-like surface. From HR-XRD measurement, we found that the crystal quality of (11-22) GaN was inferior to that of polar GaN template, which would significantly deteriorate the interfacial qualities of semipolar (11-22) InGaN/GaN QWs structure. The EL results of semipolar (11-22) LED represented lower intensity as well as broader FWHM than polar LED. It implied that non-radiative recombination centers and In localization states of semipolar (11-22) LED were much higher than those of polar LED due to the inferior crystal and structural qualities of semipolar (11-22) to polar GaN template, resulting in large blueshift of EL emission peaks. Therefore, we concluded that it is essential to improve the surface morphology and crystalline quality of semipolar (11-22) GaN template and InGaN/GaN QWs for the achievement of high power LEDs structure.

Acknowledgement

This research was supported by the IT R&D program of MKE/KEIT (10040379) and Core Corporation Research Program (2010-0026523) through the National Research Foundation of Korea (NRF) funded by the Ministry of Education, Science and Technology.

References

1. J.W. Lee, C. Sone, Y. Park, S.N. Lee, J.H. Ryou, R.D. Dupuis, C.H. Hong, and H. Kim, Appl. Phys. Lett. 95 (2009) 011108.
2. S.-N. Lee, H.S. Paeka, J.K. Son, T. Sakong, O.H. Nam and Y. Park, J. Cryst. Growth. 307 (2007) 358.
3. P. Waltereit, O. Brandt, A. Trampert, H.T. Grahn, J. Monniger, M. Ramsteiner, M. Relche, K.H. Ploog, Nature. 406 (2000) 865-868.
4. S.Y. Bea, D.S. Lee, B.H. Kong, H.K. Cho, J.F. Kaeding, S. Nakamura, S.P. DenBaars, J.S. Speck, Current. Appl. Phys. 11 (2011) 954-958.
5. T.J. Baker, B.A. Haskell, F. Wu, J.S. Speck, S. Nakamura, Jpn. J. Appl. Phys. 45 (2006) L154.
6. M. Araki, N. Mochimizo, K. Hoshino, and K., Jpn. J. Appl. Phys. 46 (2007) 555.
7. L. Lahourcade, J. Renard, B. Gayral, E. Monoroy, M. P. Chauvat, J. Appl. Phys. 103 (2008) 093514.
8. R. Armitage and H. Hirayama, Appl. Phys. Lett. 92 (2008) 092121.
9. S. -N. Lee, K.K. Kim, O.H. Nam, J.H. Kim, H. Kim, Phys. Status Solidi C 7 (2010) 2043-2045.
10. K.S. Son, D.G. Kim, H.K. Cho, K. Lee, S. Kim, K. Park, J. Cryst. Growth 261 (2004) 50-54
11. A. Lotsari, A. Das, Th. Kehagias, Y. Kotsar, E. Monroy, T.H. Karakostas, P. Gladkov, P.H. Komninou, G.P. Dimitrakopulos, J. Cryst. Growth. 339 (2012) 1-7
12. T. Detchprohm, M. Zhu, Y. Li, Y. Xia, C.Wetzel, Appl. Phys. Lett. 92 (2008) 241109.
13. T. Detchprohm, K. Hiramatsu, K. Itoh, I. Akasaki, Jpn. J. Appl. Phys. 31 (1992) L1454-L1456.
14. A.E. Romanov, T.J. Baker, S. Nakamura, J.S. Speck, J. Appl. Phys. 100 (2006) 023522.
15. B.A. Haskell, T.J. Baker, M.B. McLaurin, F. Wu, P.T. Fini, S.P. DenBaars, J.S. Speack, S. Nakamura, Appl. Phys. Lett. 86 (2005) 111917.
16. Y.-H. Cho, J.J. Song, S. Keller, M.S. Minsky, E. Hu, U.K. Mishra, S.P. Denbaars, Appl. Phys. Lett. 73 (1998) 1128.
17. D.-S. Oh, J.-J. Jang, O. Nam, K.-M. Song, S.-N. Lee, J. Cryst. Growth. 326 (2011) 33-36.
18. Z.Z. Chen, Z.X. Qin, X.D. Hu, T.J Yu, Z.J. Yang, Y.Z. Tong, X.M. Ding, G.Y. Zhang, Physica B 344 (2004) 292-296.
19. Z.C. Feng, W. Liu, S.J. Chua, J.W. Yu, C.C. Yang, T.R. Yang, J. Zhao, Thin Solid Films 498 (2006) 118-122.
20. J.-H. Chen, Z.-C. Feng, H.-L. Tsai, J.-R. Yang, P. Li, C. Wetzel, T. Detchprohm, J. Nelson, Thin. Solid. Films. 498 (2006) 123-127.
21. S.-N. Lee, J. Kim, K.-K. Kim, H. Kim, H.-K. Kim, J. Appl. Phys.108 (2010) 102813.
22. J. Bai, T. Wang, S. Sakai, J. Appl. Phys. 90 (2001) 1740.
23. B.-J. Pong, C.-H. Chen, S.-H. Yen, J.-F. Hsu, C.-J. Tun, Y.-K. Kuo, C.-H. Kuo, G.-C. Chi, Solid. State. Electronics 50 (2006) 1588-1594.
24. J. Bai, T. Wang, Y. Izumi, S. Sakai, J. Cryst. Growth. 223 (2001) 61-68.
25. N. Duxbury, U. Bangert, P. Dawson, E.J. Thrush, W. Van der Stricht, K. Jacobs, I. Moerman, Appl. Phys.Lett.76 (2000) 12.
26. X. Zhang, D.H. Rich, J.T. Kobayashi, N.P. Kobayashi, P.D. Dapkus, Appl. Phys. Lett. 73 (1998) 1430.
27. J.H. Chen, J.C. Feng, J.C. Wang, H.L. Tsai, J.R. Yang, A. Parekh, E. Armour, P. Faniano, J. Cryst. Growth. 287 (2006) 354-358.